Vol. 06, No. 02, pp. 183 –193 (2025)
ISSN: 2708-0757

JOURNAL OF APPLIED SCIENCE AND TECHNOLOGY TRENDS

www.jastt.org

Morphotectonic Controls on the Geomorphic Evolution: A Case Study of Diyala River Basin

Ayad Ali Faris Beg[1], Ghadeer F. Al-Kasoob[2], Ahmed H. Al-Sulttani[3*]

[1]*Department of Geography, College of Education, Mustansiriyah University, Baghdad, Iraq, aafbeg64@uomustansiriyah.edu.iq*
[2]*Department of Administrative and Financial Affairs, Al-Qasim Green University, Babylon 51013, Iraq, gadeerfaham@uoqasim.edu.iq*
[3]*Department of Environmental Planning, Faculty of Physical Planning, University of Kufa, Najaf, Iraq, ahmedh.alsulttani@uokufa.edu.iq*

**Correspondence: ahmedh.alsulttani@uokufa.edu.iq*

Abstract

This study investigates the influence of tectonic activity on the geomorphic evolution of the Diyala River Basin, located within variant tectonic zones (Suture, Imbricate, High-folded, and Low-folded zones) of the Arabian and Eurasian plates, and the Mesopotamia Fordeep. Spatial and topographic data, primarily derived from the SRTM v3/NASADEM with a resolution of one arc-second, were used to delineate the basin and extract key morphological parameters. A set of morphotectonic indices was calculated using ArcGIS Pro 3.4.2 to quantify tectonic signatures across the basin. The results reveal a spatial gradient in tectonic activity, with the middle and upstream sections, which are dominated by active ridges and structurally deformed landforms, showing significantly higher tectonic activity than the downstream areas. The methodology demonstrates a practical framework for assessing tectonic impacts on fluvial systems and can support broader applications in natural hazard assessment, watershed management, and regional planning. The study emphasizes the importance of integrated geomorphological analysis in identifying zones of elevated tectonic activity, particularly in structurally complex regions like the Zagros Fold-Thrust Belt.

Keywords: *Morphotectonic, Geomorphometry, Zagros Fold-Thrust Belt, GIS, Iraq*
Received: July 08th, 2025 / Revised August 19th, 2025 / Accepted: August 24th, 2025 / Online: August 25th, 2025

I. INTRODUCTION

Active tectonic processes, such as folding and faulting, accelerate river incision and impact the drainage basin through asymmetry and shifts in the river course [1]. River basins are affected by tectonic activity, which leads to changes in river shapes and regimes. Therefore, morphotectonic indices are used to assess the role of tectonic activity in the morphological evolution of river basins [2].

Geomorphological and topographic characteristics, such as subsidence and uplift, are directly related to tectonic activity in any area [3]. Therefore, analyzing and evaluating the geomorphological and morphometric characteristics of drainage networks helps in estimating and diagnosing ground deformations resulting from tectonic activity [4]. These analytical studies have begun to rely on the quantitative analysis of geomorphological indicators in their assessment of tectonic activity [5]. Geomorphological and morphometric indicators effectively help in understanding the processes that have occurred over geological time, especially concerning soil erosion and the physical properties of landforms [6-8]. In addition, these indices provide an understanding of the nature of climate, geology, and topography that control river drainage patterns. The origin and evolution of the topography can also be explained by analyzing indicators of tectonic activity in a region [9-11].

The relative activity and anomalies of river systems are challenging to track and monitor without these indicators, and these activities and anomalies are a reflection of tectonic activity [12]. The characteristics of the drainage network in a basin are controlled by the geological structure and composition [13]. Tectonic activity is one aspect of geology, along with lithology and structure, and is one of the processes that control morphotectonic changes within a drainage basin, affecting the evolution and continuous modification of the topography [14, 15]. Observed changes in the drainage network, including channel migration and river channel meandering, can provide inferences about tectonic activities in a region [16].

doi: 10.38094/jastt62352

In addition, Geographic Information Systems (GIS) applications are practical and efficient in these types of problems and all areas of spatial management and planning, due to the processing and modeling of data they provide. Morphometric and morphotectonic analyses are complex problems that require large spatial data, and GIS can contribute to their analysis and modeling [13]. The importance of the Digital Elevation Model (DEM) lies in its ability to provide a mathematical and quantitative representation of ground features, showing the surface response to internal movements and accompanying distortions at any map scale [17].

The current study was conducted in the Diyala River Basin, which is an important basin because it is one of the major basins feeding the Hamrin Dam Lake. The basin spans multiple geological settings, crossing diverse formations and structures. Most of the source area lies in the Zagros Fold-Thrust Belt, where geological structures such as folds and faults, in addition to tectonic activity, extend to the Mesopotamian Plain. The study aims to analyze and evaluate the variability of tectonic activities and their impact on the geomorphological evolution of the basin, providing valuable insights into the geology and internal and external geomorphological processes that control basin morphology. This analysis uses various morphotectonic indicators and developed GIS techniques.

II. Description Of The Study Area

The Diyala River Basin extends from Iranian lands located on the boundary between the Arabian and Eurasian plates to the Mesopotamian plain. It flows in a northeast-to-southwest direction through Iraqi lands, encompassing the Diyala, Salah al-Din, and Baghdad governorates. The river feeds the lake of Hamrin Dam and is connected to the Tigris River in the south of Baghdad governorate.

Geographically, the basin is bounded between latitudes 33° 12' 48.22" - 35° 43' 38.86" N and longitudes 44° 19' 16.21" - 47° 57' 30.38"E, and covers an area of approximately 32248.3 square kilometers (Figure 1).

Geologically, in the eastern parts of the basin, basic plutonic, clastic, metamorphic, siliciclastic sedimentary, and carbonate sedimentary rocks are exposed. In contrast, most of the middle parts are covered by mixed and carbonate sedimentary rocks, and Quaternary deposits cover the downstream area of the basin.

Structurally, the basin lies across several tectonic zones of the Zagros Fold-Thrust Belt, including (Suture, Imbricate, High-folded, and Low-folded zones) of the Arabian and Eurasian plates, and extending into the Mesopotamia Fordeep [18, 19]. This structural gradient is reflected in the density of faults and folds and the NW–SE orientation of the structural ridges in the center and east, contrasted with the diminishing structural features towards the southwest. This structural arrangement explains the increased indicators of tectonic activity upstream compared to downstream (Figure 2a) [20]. The basin is characterized by topographic diversity, featuring mountainous regions in the east, as well as plateaus and plains in the center and western parts of the basin. The height of the eastern region reaches approximately 3,300 meters above sea level (Figure 2b).

The climate of the basin is classified into three zones. The northern parts have a semi-humid or moderate climate, the second zone is semi-dry, and the middle parts are semi-arid. The southern parts are classified as a dry climate [21].

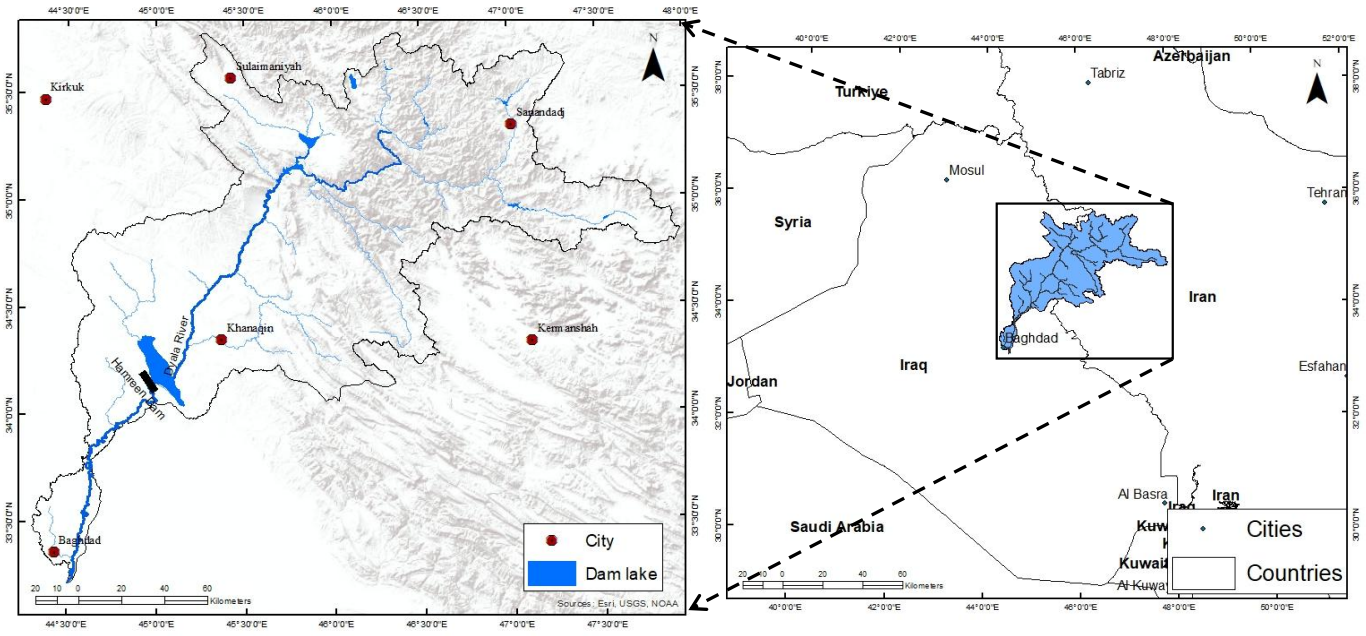

Fig. 1. Location map of Diyala River Basin

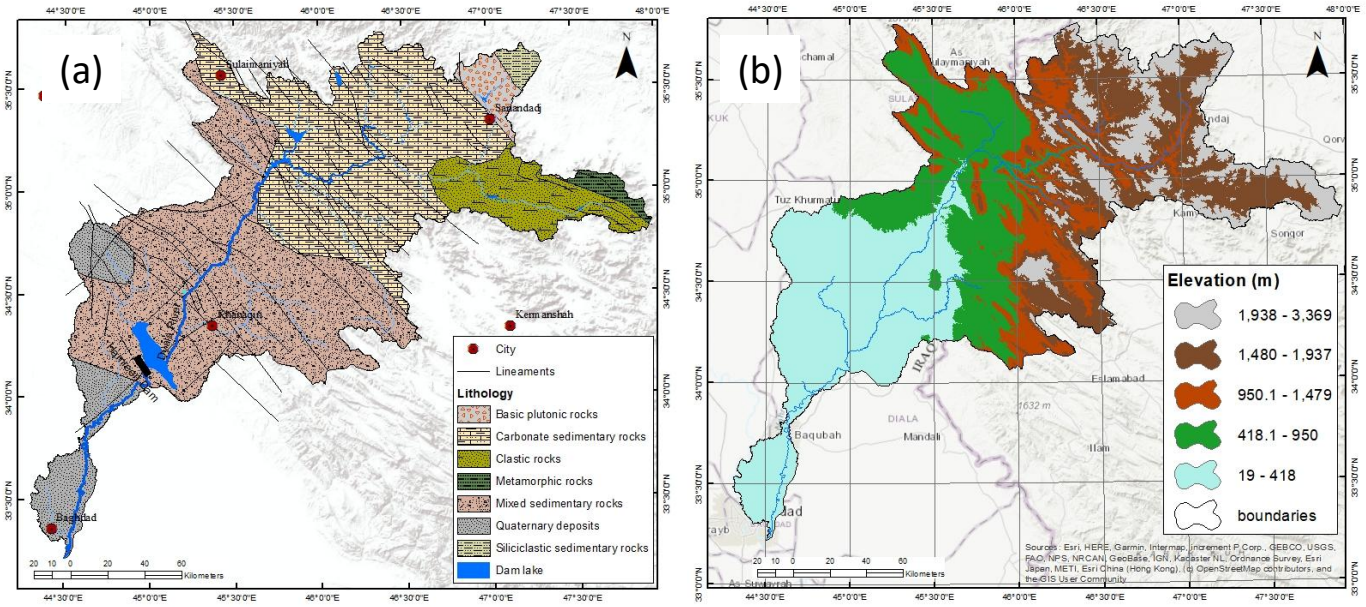

Fig. 2. Maps of the Diyala River Basin: a) Geological and structure map, b). Distribution of elevation levels.

III. MATERIALS AND METHODS

The SRTM v3/NASADEM product was used with a resolution of 1 arc-second (fill-enhanced version), and all raster images were reprojected to UTM 38N – WGS84 to ensure consistent metric measurements. Data processing and calculation of indicators were done using ArcGIS Pro 3.4.2 software to assess the tectonic influence on the morphological characteristics of the basin.

Indices were calculated at the basin scale with cross-sectional measurements along the main stream (SL and RSI), and on multiple mountain front sections for the Smf index. Asymmetry indices (Af/Tf) were evaluated across the basin. These selections were made to highlight structural-lithological contrasts. The morphotectonic indices were calculated and extracted, which are including: Mountain Front Sinuosity (Smf), Stream length-gradient index (SL), Knick points, Transverse topographic asymmetry factor (Tf), Drainage Basin Asymmetry (Af), River sinuosity index (RSI), Slope index (Si), Hypsometric Integral (HI) and Index of Active Tectonics (IAT).

A. *Mountain front sinuosity (S_{mf})*

The mountain front sinuosity (Smf) index is used to identify active and inactive mountain fronts. It can be calculated by dividing the length of the mountain front by the straight-line length, as in the following formula [10, 22].

$$S_{mf} = (\frac{L_{mf}}{L_s}) \text{……..(1)}$$

Where L_{mf} is the length of the mountain front, L_s is the straight distance between the endpoints of the mountain front. If the Smf value is less than 1.4, it means the mountain front is most tectonically active, but if it is higher than 3, it means inactive mountain fronts [22, 23]

B. *Transverse topographic asymmetry factor (T_f)*

This index gives an important indication of the degree of symmetry of the basin, the value of T_f ranges between 0 for a perfect symmetrical basin, and 1 for a very asymmetrical basin that common in basins with a dendritic drainage pattern or where the basin subjected to a differential tectonic activity on both sides of the main channel [22, 24]. The Tf index can be calculated from the following formula:

$$T_f = (\frac{D_a}{D_{md}}) \text{ ……. (2)}$$

Where D_a is the distance from the main valley channel to the basin midline, D_{md} is the distance from the basin boundary to the basin midline.

C. *The drainage basin asymmetry index (Af)*

The asymmetry index identifies the slope of the basin away from the main stream channel, which is caused by tectonic impacts that result in elevation variations on both sides of the drainage basin. Af is calculated as follows [25, 26]:

$$Af = A_r/A_t \times 100 \text{ ……. (3)}$$

While Pérez-Peña, Azor, Azañón and Keller [1] give an alternative formula as shown:-

$$Af = \left|50 - \frac{A_r \times 100}{A_t}\right| \text{ ……(4)}$$

Where Ar is the right-side area of the basin for the main channel, At is the total area of the drainage basin.

D. *Stream length-gradient index (SL)*

SL measures a river's ability to erode the bed and transport sediment [27]. The index values are high for rivers that pass through resistant rocks that have been subjected to tectonic

uplift, while they decrease for rivers that pass over fragile rocks or flow along strike-slip faults [22, 24, 28].

$$SL = \frac{\Delta H}{\Delta L} \times L \quad \ldots\ldots\ldots\ldots (5)$$

Where L is the length from the highest point on the river channel to the reach midpoint, ΔH/ΔL is the slope over that portion of the channel where the reading is taken. If SL< 300 (1: Inactive), 300<SL<500 (2: Semi active), and 500< SL(3: Active) [11, 27].

E. Knickpoints

Knickpoints along the longitudinal profile of the main stream were identified semi-automatically by extracting local dip breaks using a moving window and then visually checking sections that cut through resistant rock edges. It is also defined as abrupt changes in river slope or channel profile with a similar slope along both sides of the knickpoint [29]. There are several reasons for the formation of knickpoints, including differences in rock resistance, structural features such as faults and joints, tectonic deformation of the riverbed, local erosion, and possibly due to sedimentary inputs from tributaries or hill slopes [30].

F. River sinuosity index (RSI)

RSI is used to identify whether a basin is close to equilibrium. If the RSI value increases, it is referred to as low-tectonic activity (Baharvand, 2022). It also indicates the deviation of the stream from a straight to a meandering course [31].

$$RSI=C/V \quad \ldots\ldots\ldots\ldots (6)$$

Where C is the real stream section length, and V is the typical straight length of the section. If the RSI value is greater than 1.3 (1: inactive), 1.15 -1.3 (2: semi-active), or less than 1.15 (3: active) (Baharvand, 2022).

G. Slope index (Si)

Si is measured by dividing the height difference between two points along the river channel by the horizontal distance between them. The steep slope indicates active faulting or uplift due to tectonic activity [32].

H. Hypsometric analysis

It is the study of horizontal sections of the area at a specific elevation [33]. The relationship between the relative area and the relative elevation is plotted on the x-axis (relative area) and y-axis (relative elevation) as a hypsometric curve, and the stage of geomorphic development of the basin is estimated based on the Hypsometric Integral (HI) [7]. Hypsometric analysis was carried out using the morphometric toolbox developed by the first author [34].

IV. Results and Discussion

The results of morphotectonic analysis show the impacts of tectonic activities on the morphological development of the Diyala River Basin as follows:

A. Mountain Front Sinuosity (S_{mf})

The values of Mountain Front Sinuosity (Smf) were measured at twenty-nine sections of mountain fronts. Figure 3a and Table I show that, three sections, B, E, and QQ are tectonically inactive with value greater than 3.0 located along the slopes characterized by dendritic drainage pattern, whereas, Seven sections come in semi active status i.e., sections A, D, F, G, I, K, and OO with S_{mf} values ranged from 1.435 to 2.765, these sections are located at the mountain fronts covered by rocks and deposits with more resistance to erosion, while the other sections are shows active fronts with S_{mf} values less than 1.4, these sections are located at front of tectonic mountains and ridges with high resistance to erosion processes. The measured sections demonstrate the interaction balance between erosion processes and tectonic activities along mountain fronts, with most of the basin area affected by semi-active to active tectonic processes.

TABLE I. Measurements Of Sinuosity And Straight Lengths In Kilometers, And Calculated Mountain Front Sinuosity (Smf) Values At Different Mountain Front Sections

Section	Sinuosity length (km)	Straight length (km)	Mountain Front Sinuosity (Smf)	Class	Section	Sinuosity length (km)	Straight length (km)	Mountain Front Sinuosity (Smf)	Class
A	16.9	11.8	1.435	2	DD	50.8	42.7	1.19	3
B	13	4.2	3.139	1	EE	27.5	21.5	1.281	3
C	33.3	26.6	1.255	3	FF	25.7	22.6	1.138	3
D	31.3	17	1.837	2	GG	20.4	19	1.077	3
E	142.2	10.6	13.449	1	HH	27.9	27.4	1.018	3
F	24.2	14.6	1.657	2	II	28.4	26.3	1.083	3
G	38.2	16.3	2.345	2	JJ	14.8	14.1	1.047	3
H	12.5	11.8	1.061	3	KK	30.8	27.8	1.108	3
I	10	4.2	2.389	2	LL	34.7	25.3	1.371	1
J	5.9	5.5	1.06	3	MM	14.5	13.6	1.071	3
K	12.1	4.4	2.765	2	NN	19.5	18.4	1.059	3
L	8	6.9	1.162	3	OO	55.4	24.6	2.253	2
AA	40.5	33.7	1.202	3	PP	31.7	25.6	1.235	3
BB	37.1	33.5	1.107	3	QQ	105.8	31.3	3.384	1
CC	69.6	59.7	1.166	3					

B. Transverse topographic asymmetry factor (T_f)

To assess the tectonic tilt of the Diyala River basin, seven sections at different locations in the basin were selected to calculate T_f as shown in Figure 3b and Table II. The basin shows a high degree of tectonic tilt at sections A, D, and G, with Tf values ranging from 0.6 to 0.91. In contrast, sections C and E show moderate asymmetry with values of 0.31 and 0.43, respectively, while sections B and F have Tf values of 0.19 and 0.10, respectively. They are prone to being highly symmetric and very slightly affected by tectonic tilt.

C. The drainage basin asymmetry index (Af)

According to the formula used by Cox [26], a basin with an Af value of 59.54 indicates that the basin is tilted. According to Pérez-Peña, Azor, Azañón and Keller [1], $|Af - 50| \approx 9.54$ indicates a right-tilted basin, and because the basin falls into the gently asymmetric class 9.54 (Figure 3b and Table II).

TABLE II. TRANSVERSE TOPOGRAPHIC ASYMMETRY FACTOR (TF) VALUES AT DIFFERENT SECTIONS AND DRAINAGE BASIN ASYMMETRY (AF) OF THE MAIN BASIN.

Sections	Line ID	Length (km)	Index Formula	Index value	Class
Length of main channel	0	390.4			
Sec. A	1	33.4	$T_f = (D_a \div D_{md})$	0.77	2
	2	43.2			
Sec. B	3	7.2		0.19	1
	4	37.3			
Sec. C	5	33.7		0.31	1
	6	110.2			
Sec.D	7	36.9		0.60	2
	8	61.3			
Sec. E	9	19.0		0.43	1
	10	44.1			
Sec. F	11	5.2		0.10	1
	12	53.2			
Sec. G	13	20.4		0.91	2
	14	22.5			
			Index Formula	***Af value***	
Right side area (km2)	19200.49		$Af = A_r \div A_t \times 100$	59.54	1
Total basin area(km2)	32248.29		$Af = 50 - \frac{A_r \times 100}{A_t}$	9.54	2

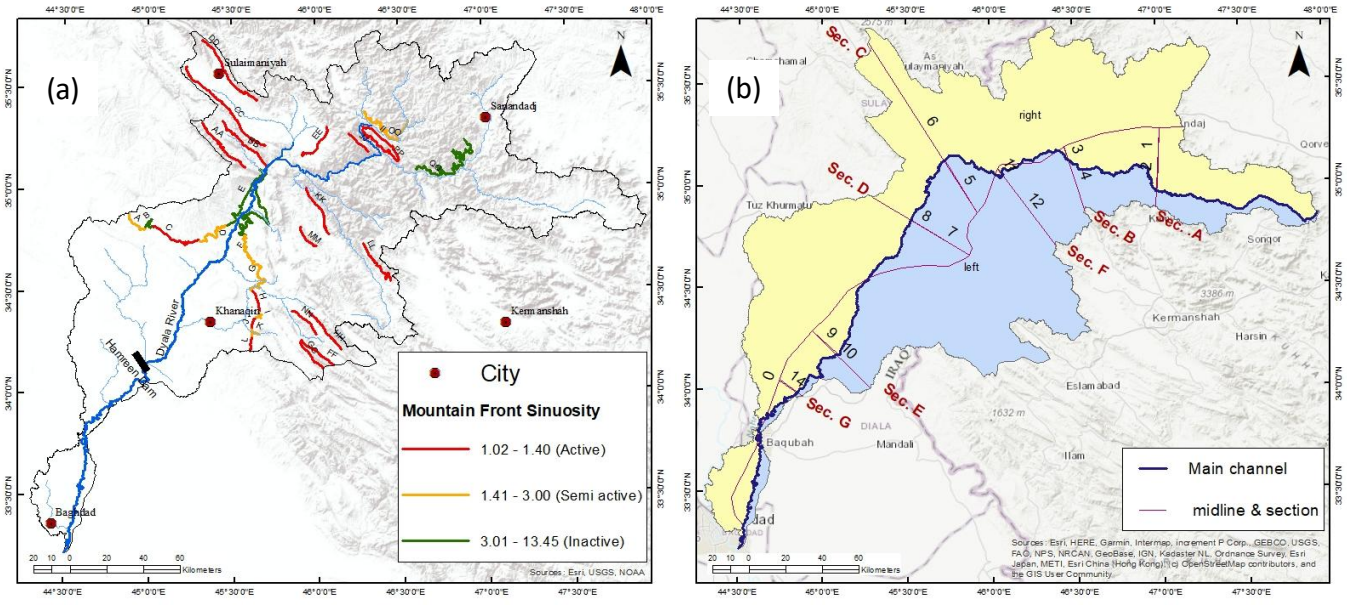

Fig. 3. Maps of morphotectonic measurements a). Mountain front sinuosity, b). Transverse topographic asymmetry factor (Tf)

D. Stream length-gradient index (SL)

The main channel route is divided into three sections, as illustrated in Figure 4 and summarized in Table III. From Figure 2a, in Section 2, where the primary channel intersects carbonate sedimentary rocks within the active zone, SL is expected to be elevated and frequently exhibits sharp local peaks (knick-zones) due to the steepening of resistant beds or structures, which in turn signal higher stream power and focused incision. In Section 1, siliciclastic clastics (sandstone–siltstone–shale) are encountered, with moderate to lower SL overall, punctuated by local spikes where tougher sandstones or faults are encountered. In Section 3, mixed sedimentary units grading to Quaternary alluvium downstream, SL typically declines as gradients ease and the channel meanders on softer/alluvial substrates. In short, resistant carbonate/bedrock reaches (and uplift) high/sloping SL with knickpoints; weaker clastics-alluvium, smoother SL, consistent with the classic use of SL to flag lithologic/tectonic anomalies along.

E. Knickpoints

Many knickpoints are recognized along the main stream channel section, as shown in Figure 4. All the Knickpoints are found where the stream crosses through rock outcrop ridges, where the presence of successive rock layers of varying hardness produces a varied stream slope that represents the suture zone.

F. River sinuosity index (RSI)

As for the state of straightness or meander of the stream, it is divided into the following categories: if RSI is less than 1.1 (straight), 1.1 to 1.5 (deviant), or if it is greater than 1.5 (meander), as shown in Figure 5 and Table IV [31, 35].

TABLE III. STREAM LENGTH-GRADIENT INDEX (SL)

Sec. no.	ΔH	Δl	L	SL	Class
Sec.1	672	85000	47000	371.5	2
Sec.2	770	112000	204000	1402.5	3
Sec.3	302	175000	392000	676.5	2

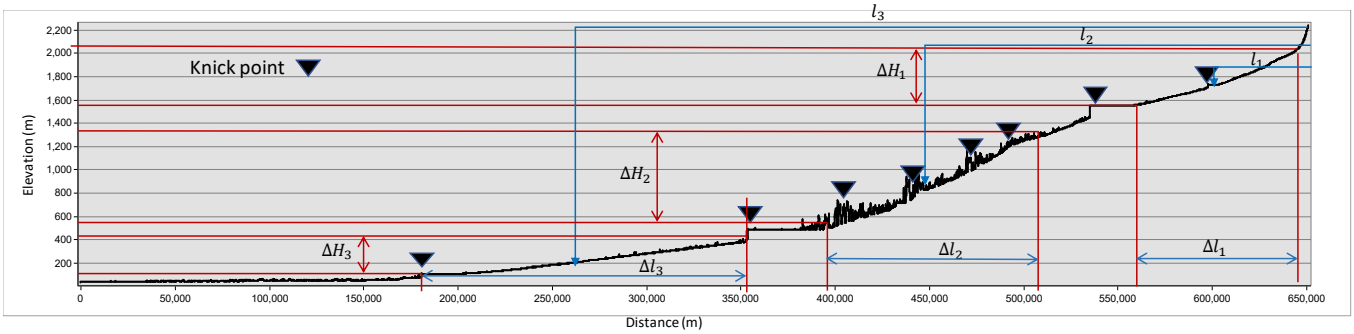

Fig. 4. Measurements of stream length-gradient index (SLG) along the main channel route with Knickpoints locations.

TABLE IV. REAL, TYPICAL LENGTHS OF MAIN STREAMS AND RIVER SINUOSITY INDEX VALUES.

Id	Real stream length (c) (meters)	Typical length (v) (meters)	River sinuosity index (RSI)	Class of active tectonic	Class of stream straightness
1	78195.84	59094.07	1.32	1	deviant
2	69071.08	36030.07	1.92	1	meander
3	16140.03	15037.04	1.07	3	straight
4	35241.40	22739.27	1.55	1	meander
5	40479.62	34365.83	1.18	2	deviant
6	28844.39	24011.01	1.20	2	deviant
7	20275.58	15343.97	1.32	1	deviant
8	30157.93	25660.99	1.18	2	deviant
9	69789.79	38214.40	1.83	1	meander
10	52240.89	38280.70	1.36	1	deviant
11	51552.59	38521.24	1.34	1	deviant
12	37610.71	19494.02	1.93	1	meander
13	56905.33	45946.24	1.24	2	deviant
14	91210.87	67973.50	1.34	1	deviant
15	110298.95	62554.16	1.76	1	meander
16	99081.06	78413.08	1.26	2	deviant
17	66709.89	52717.18	1.27	2	deviant
18	100886.49	45433.80	2.22	2	meander
19	73135.47	50583.54	1.45	1	deviant
20	48911.18	19502.88	2.51	1	meander
21	40173.51	30428.83	1.32	1	deviant
22	49685.12	37734.21	1.32	1	deviant
23	29863.49	26730.98	1.12	3	deviant
24	41571.74	30594.94	1.36	1	deviant
25	30497.24	21867.50	1.39	1	deviant
26	19522.85	18727.69	1.04	3	straight
27	24435.67	21399.51	1.14	3	deviant
28	28647.20	23760.34	1.21	2	deviant
29	10558.37	10117.85	1.04	3	straight
30	40499.08	29077.71	1.39	1	deviant

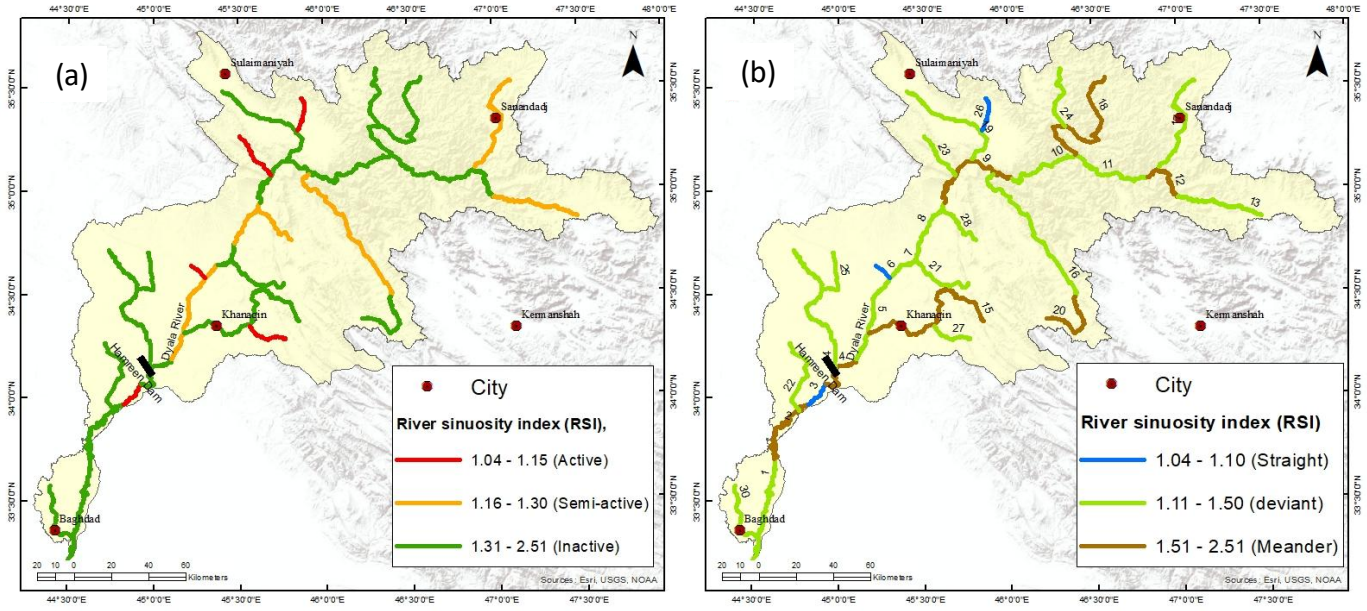

Fig. 5. Maps of River Sinuosity Index (RSI), a). RSI values based on activity, b). RSI values based on river straightness or meander

G. Slope index (Si)

Based on Zinck [36] method of slope classification, five slope classes are identified in the Diyala River basin. Specifically, 48.8% of the middle and upper parts of the basin are classified as rolling, steeply dissected, or mountainous. This area is geologically characterized by numerous rock outcrops exposed as ridges of anticlines extending in a NW-SE direction, crossing the flow direction of the main streams in the basin. In contrast, the rest of the downstream area of the basin has almost flat to undulating topography, covered by mixed sedimentary rock and Quaternary deposits, with some gentle slope ridges crossing the area (Figure 6 and Table V).

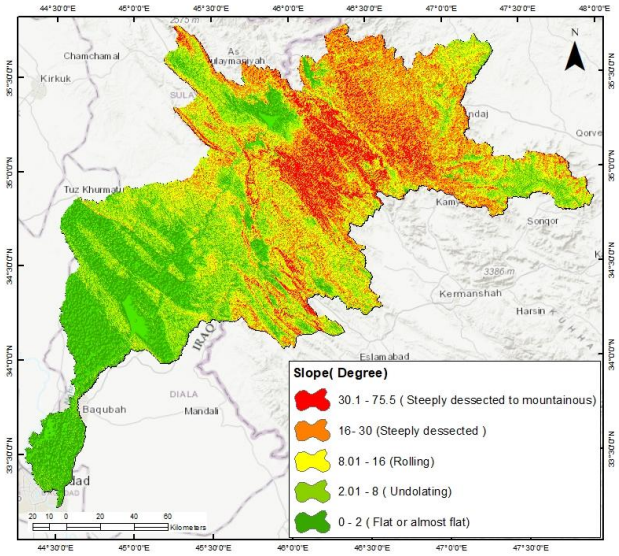

Fig. 6. Slope classes of the Diyala River basin according to Zinck (1988).

TABLE V. SLOPE CLASSES, AREA, AND PERCENTAGE OF EACH CLASS BASED ON ZINCK [36] CLASSIFICATION.

Shape class	Slope	Area(km^2)	Area(%)	Class
Flat or almost flat	0 - 2	8151.6	25.3	1
Undulating	2.01 - 8	8350.0	25.9	2
Rolling	8.01 - 16	5634.0	17.5	3
Steeply dissected	16- 30	7362.1	22.8	4
Steeply dissected to mountainous	30.1 - 75.5	2750.6	8.5	4

H. Hypsometric analysis

The results of hypsometric analysis curried out based on Strahler classification; indicate the basin pass in monadnock stage of geomorphic development, with HI value about 30 that mean the basin landscapes have been more eroded, and the upper part of the hypsometric curve shows a convex shape above the volumetric curve that indicate may be the landscape in this part of basin may be related to uplift in geological structures produced high landscapes (Figure 7 and Table VI). While the hypsometric curve is concave in the downstream part of the basin and lies slightly below the volumetric curve, this indicates that no deposition has occurred in this area, and most of the sediment is transported out of the basin.

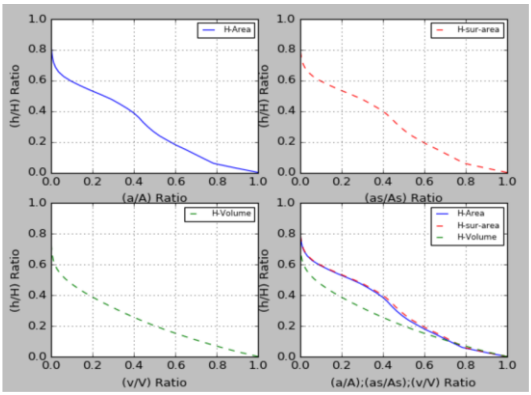

Fig. 7. Hypsometric and volumetric curves of the Diyala River Basin

I. The Index of Active Tectonics (IAT)

The Index of Active Tectonics (IAT) is used to get an integrated idea about the influence of tectonic activities in delineating the morphology of the basin, as expressed by the following equation:-

$$IAT = \frac{S}{N} \text{.....(7)}$$

Where S is the summation of used index classes, and N is the number of indices. Many authors divided the value of IAT into four activity classes, i.e., very high (1.0 - 1.49); high (1.5 – 1.99); moderate (2.0 - 2.49); and low ($IAT \geq 2.5$) (Table VII) [5, 37, 38].

TABLE VI. RELATIVE HEIGHT, AREA, SURFACE AREA, AND VOLUME VALUES OF HYPSOMETRIC AND VOLUMETRIC CURVES.

*Relative height(h/H)	*Relative area(a/A)	** Relative surface area (as/As)	** Relative volume (vol/VOL)
0	1	1	1
0.02979	0.8875	0.89306	0.90566
0.05958	0.78391	0.79447	0.822
0.08937	0.7385	0.75104	0.74561
0.11916	0.69447	0.70879	0.67391
0.14896	0.6502	0.6661	0.60624
0.17875	0.60268	0.61984	0.54355
0.20854	0.56255	0.58028	0.48511
0.23833	0.52373	0.54167	0.43068
0.26812	0.49282	0.5103	0.37977
0.29791	0.46694	0.48359	0.33167
0.3277	0.44399	0.45968	0.28602
0.35749	0.42396	0.43851	0.24251
0.38728	0.39953	0.41295	0.20111
0.41708	0.36775	0.38006	0.16256
0.44687	0.33125	0.34239	0.1275
0.47666	0.29189	0.30176	0.09622
0.50645	0.24245	0.25111	0.06936
0.53624	0.18948	0.19685	0.04769
0.56603	0.14057	0.14661	0.03119
0.59582	0.09612	0.10099	0.01936
0.62561	0.06093	0.06466	0.01158
0.6554	0.03667	0.03935	0.00678
0.6852	0.0218	0.02362	0.00391
0.71499	0.01269	0.01388	0.00222
0.74478	0.00748	0.00824	0.00123
0.77457	0.0043	0.00477	0.00065
0.80436	0.00236	0.00264	0.00033
0.83415	0.0012	0.00136	0.00016
0.86394	0.00061	0.00069	0.00007
0.89373	0.00029	0.00033	0.00003
0.92353	0.00011	0.00012	0.00001
0.95332	0.00002	0.00003	0
0.98311	0	0	0
1	0	0	0
Minimum Height =19.0 m			
Maximum Height =3369.0 m			
Incremental Elevation Interval =100 m			
Total Basin Height (H) =3350.0 m			
Hypsometric Integral =29.6			
**Surface area Hypsometric Integral=30.35			
**Volumetric Integral =22.90			

[a.] Source: * after Strahler [7], and **after Beg [39]

The calculated values of IAT provided an integrated understanding of the tectonic activity's impact on the Diyala River basin. The IAT value indicates that the basin experienced high to moderate active conditions. Most of the basin area subjected to active tectonic processes is located in the middle and upstream regions, which are situated in the suture zone between the Arabian and Eurasian plates (the convergence boundary). In contrast, the downstream area is prone to being inactive tectonically, and no tectonic landforms appear in this area.

The inferred spatial pattern—higher activity in structurally rugged headwater areas and gradual downstream retreat—is consistent with studies in fold-thrust belts and mountainous basins, where low Smf values, high SL, and frequent knickpoints are associated with more resistant lithology and active structures. The concordance of the indices in the Diyala Basin (low Smf with high SL and decreasing fluvial undulations where gradients are steep) supports the interpretation that the topographic gradient is mainly caused by tectonic activity rather than climatic.

Some studies have addressed the Diyala Basin in the field of morpho-tectonics and morphometry, adopting different analytical methods. Aziz, Abdulrazzaq and Mansur [40] applied HC/HI analysis and its statistical moments to 26 sub-basins in Diyala and concluded that concave dominates and HI values are small, with higher uplift in the north/northeast compared to the south/southwest. The observed spatial uplift direction (north/northeast to south/southwest) is consistent with our pattern shown by the SMF/SL indices and the frequency of knickpoints. The study focused on HC/HI indicators without cross-sectional measurements on mountain fronts or the mainstream and SL.

The study by Kadhim and Al-kubaisi [41] presents a combined procedure for measuring relative tectonic activity using LRTI (combining morphometric indices with lithological strength and AHP/FAHP weightings). The study categorized the resulting data into five categories, highlighting that ZM and SR in the northeast of the basin are “very high,” and KU and HM in the southeast of the basin are “very low.” The LRTI maps qualitatively match our pattern (higher activity northeast), supporting the reliability of our Smf/SL

inferences. The study relies on weights and estimated thresholds (AHP/FAHP), which expose the values to a degree of subjectivity. Furthermore, the method is complex and difficult to reproduce without the same matrices and weightings. Where the present a transparent and reproducible alternative: classical threshold-based indices, with cross-sectional measurements on mountain and stream interfaces, revealing "where and why" activity is most intense, without relying on subjective weightings.

TABLE VII. VALUES OF MORPHOTECTONIC INDICES AND THE INDEX OF ACTIVE TECTONIC VALUES.

Basin	Classes of morphotectonic indices								Activity class
	Mountain Front Sinuosity (Smf)	Stream length-gradient index (SL)	Transverse topographic asymmetry factor (Tf)	drainage basin asymmetry index (Af)	River sinuosity index (RSI)	Slope index (Si)	Hypsometric integral (HI)	Index of Active Tectonics (IAT)	
Diyala River basin	3	2.3	2	1.4	1.7	3	1	2.05	Moderate active (Class 3)

V. CONCLUSIONS

The results of the morphotectonic analysis in this study clearly indicate the increasing influence of tectonic activity on shaping the morphology of the Diyala River Basin, particularly toward the northeastern regions of the basin, where the upper headwaters are located. The indicators used, such as the mountain-front sinuosity (Smf), the mountain front slope index, and the basin shape index, among others, revealed a gradual increase in the intensity of tectonic activity from the center of the basin toward the northeastern edges, reflecting an active and entrenched tectonic pattern in this part of the basin. This increased tectonic activity is directly attributed to the geological location of the upper streams area, which lies on the highly active collision/convergence boundary of the Arabian and Eurasian plates, within the Zagros Fold-Thrust Belt. This tectonically active region in Iraq and the surrounding areas, with the highest rates of modern deformation recorded, contributes to accelerated geomorphological changes.

The results confirm that the structural-lithologic gradient across the Diyala Basin is the main determinant of the variability of morphotectonic indicators. Low Smf values, high SL values, and the abundance of upstream knickpoints are consistent with active orogenic interfaces and fold-thrust structures. Therefore, the interaction of geomorphological and geological data with morphotectonic analysis provides an efficient spatial approach to detecting indicators of tectonic deformation, enabling a comprehensive understanding of the basin's recent geodynamic evolution. This conclusion contributes to a practical framework for identifying tectonic hazard zones and guiding risk management, hydrology, and regional and urban planning in the Zagros Belt and its nearby areas.

In light of the findings, this study recommends expanding the scope of the analysis to include other valleys and basins located within the Zagros Fold-Thrust Belt, with a focus on studying the spatial variation in the impact of tectonic activity and identifying areas with a high potential for structural deformation and tectonic hazards across this structurally active region. Such future studies will contribute to building an accurate spatial database that supports decision-makers in the areas of sustainable development and regional planning based on solid geological and geomorphological foundations.

Throughout the Zagros Fold-Thrust Belt, our multi-index signals are consistent with, but locally stronger than, neighboring case studies. Along the Khanaqin fault zone, the Bamo Anticline exhibits moderate activity, with IRAT classes of 38% high, 56% moderate, and 6% low, and uniformly moderate mountain-front sinuosity (Smf = 1.12-1.27) [42]. In the Kifri Chai Basin, a composite IAT of 2.35 (class 3, moderate) and an average Smf of $\approx$ 1.8 also indicate weak front-scale activity with localized enhancements [43] (Elias et al., 2019). In contrast, many of the Diyala fronts fall into the semi-active to active categories, and our channel metrics include SL anomalies within the same regionally recognized "active" range (SL > 500), comparable to the Dukan area, where SL peaks reach around 769 [44]. Basin-scale hypsometry also supports this view: a HI $\approx$ 0.30 places the Diyala as more dissected than the adjacent Al-Adhaim Basin (HI $\approx$ 0.19; Monadnock Stage) [33], but within the 0.16-0.53 range previously reported across the Diyala subbasins, where elevation increases northeastward. In conclusion, the Diyala shows a broader spectrum of activity—from straight sections with low Smf and high SL reaches to mature/old subbasins, consistent with stronger structural segmentation across the suture domains.

As limitations, although SRTM v3/NASADEM void-filling improves elevation completeness, residual vertical errors and canopy effects can affect some morphometric elevation-based indices.

REFERENCES

[1] J. V. Pérez-Peña, A. Azor, J. M. Azañón, and E. A. Keller, "Active tectonics in the Sierra Nevada (Betic Cordillera, SE Spain): Insights from geomorphic indexes and drainage pattern analysis," *J Geomorphology,* vol. 119, no. 1-2, pp. 74-87, 2010. https://doi.org/10.1016/j.geomorph.2010.02.020.

[2] M. Ezati, and M. Agh-Atabai, "Active tectonic analysis of Atrak river subbasin located in NE Iran (East Alborz)," *J J Tethys,* vol. 1, pp. 177-188, 2013.

[3] R. Dubey, and G. P. Satyam, "Morphotectonic appraisal of Yamuna river basin in headwater region: a relative active tectonics purview," *Journal of the Geological Society of India,* vol. 92, no. 3, pp. 346-356, 2018. https://doi.org/10.1007/s12594-018-1090-5.

[4] A. K. Anand, and S. P. Pradhan, "Assessment of active tectonics from geomorphic indices and morphometric parameters in part of Ganga basin," *J*

Journal of Mountain Science, vol. 16, no. 8, pp. 1943-1961, 2019. https://doi.org/10.1007/s11629-018-5172-2.

[5] M. Pourali, R. Hoseynzadeh, and M. Akbari, "Quantitative analysis of relative active tectonics using geomorphic indices in Band-Golestan basin, northeastern Iran," *J Spatial Information Research,* vol. 28, pp. 419-429, 2020. https://doi.org/10.1007/s41324-019-00303-y.

[6] S. Bhatt, R. Singh, M. Ansari, and S. Bhatt, "Quantitative Morphometric and Morphotectonic Analysis of Pahuj Catchment Basin, Central India," *Journal of the Geological Society of India,* vol. 96, no. 5, pp. 513-520, 2020. https://doi.org/10.1007/s12594-020-1590-1.

[7] A. N. Strahler, "Hypsometric (Area-Altitude) Analysis of Erosional Topography," *Geological Society of America Bulletin,* vol. 63, no. 11, pp. 1117, 1952. https://doi.org/10.1130/0016-7606(1952)63[1117:HAAOET]2.0.CO;2.

[8] R. E. Horton, "Erosional Development of Streams and Their Drainage Basins; Hydrophysical Approach to Quantitative Morphology," *Geological Society of America Bulletin,* vol. 56, no. 3, pp. 275, 1945. https://doi.org/ 10.1130/0016-7606(1945)56[275:EDOSAT]2.0.CO;2.

[9] S. Shekhar, Y. Mawale, P. Giri, R. Jaipurkar, and N. Singh, "Remote Sensing and GIS Based Extensive Morphotectonic Analysis of Tapti River Basin, Peninsular India," *Journal of Scientific Research,* vol. 65, no. 3, 2021. https://doi.org/10.37398/JSR.2021.650304.

[10] A. Khalifa, B. Bashir, A. Alsalman, and N. Öğretmen, "Morpho-tectonic Assessment of the Abu-Dabbab Area, Eastern Desert, Egypt: Insights from Remote Sensing and Geospatial Analysis," *ISPRS International Journal of Geo-Information,* vol. 10, no. 11, pp. 784, 2021. https://doi.org/10.3390/ijgi10110784.

[11] S. Baharvand, "Analysis of Tectonic Activity using Morphotectonic Indices (Case study: Kesmat Basin, Lorestan Province, Iran)," *J Geotechnical Geology,* vol. 18, no. 1, pp. 643-647, 2022.

[12] P. Singh, K. Prakash, S. Kumar, A. K. Kannaujiya, and T. Mohanty, "A synergistic approach to morphotectonic evolution for watershed management in the Bearma River Basin, Central India," *J Journal of Hydroinformatics,* vol. 25, no. 5, pp. 1822-1843, 2023. https://doi.org/10.2166/hydro.2023.055.

[13] S. C. Bhatt, A. Patel, P. Srivastava, V. K. Singh, M. Singh, and S. K. Singh, "A GIS-based morphometric and morphotectonic analysis of Johilla River Basin, Central India," *Geospatial Technologies for Integrated Water Resources Management: Mapping, Modelling, and Decision-Making*, pp. 49-64: Springer, 2024. https://doi.org/10.1007/978-3-031-57777-2_4.

[14] R. Sharma, Y. Singh, Rajwant, N. Singh, J. N. Malik, M. Dhali, E. Srivastava, and N. Sharma, "Appraisal of Active Tectonics: An Insight from the Morphotectonic Study of Drainage Basins and OSL Dating in the Kangra Area, Himachal Pradesh," *Journal of the Geological Society of India,* vol. 100, no. 7, pp. 996-1006, 2024. https://doi.org/10.17491/jgsi/2024/173942.

[15] A. K. Al-Ali, and R. M. Amin, "Tectonic Evaluation by Using Morphotectonic Indices at Zurbatiyah Area, Eastern Iraq," *Iraqi Geological Journal*, pp. 18-39, 2025. https://doi.org/10.46717/igj.2025.58.1D.2.

[16] H. Deopa, and M. J. A. J. o. G. Resmi, "Quantification of geomorphic signatures of neotectonic activity within the Khoh River Basin: a geospatial approach," vol. 18, no. 6, pp. 1-16, 2025. https://doi.org/10.1007/s12517-025-12265-7.

[17] P. Gahlaut, R. C. Patel, R. Ayyamperumal, M. Sati, and D. C. Nainwal, "Assessment of Recent Tectonic Activity along the Yamuna Basin, Garhwal Region, NW-Himalaya, India: Based on Morphotectonic Analysis," *Open Journal of Geology,* vol. 11, no. 12, pp. 734-755, 2021. https://doi.org/10.4236/ojg.2021.1112036.

[18] S. F. Fouad, "Tectonic map of Iraq, scale 1: 1000 000, 2012," *Iraqi Bulletin of Geology and Mining,* vol. 11, no. 1, pp. 1-7, 2015.

[19] Y. Mustafa, "Spatiotemporal analysis of vegetation cover in Kurdistan region-Iraq using MODIS image data," *Journal of Applied Science and Technology Trends,* vol. 1, no. 1, pp. 01-07, 2020. https://doi.org/10.38094/jastt119.

[20] M. Ghorbani, M. Ghorbani, and Metamorphism, "Faults and tectonic phases of Iran," *The Geology of Iran: Tectonic, Magmatism*, pp. 81-149, 2021. https://doi.org/10.4236/ojg.2021.1112036. https://doi.org/10.1007/978-3-030-71109-2_3.

[21] O. S. Al-Tamimi, and S. A. A. Gamel, "The Climatic Regions and Desertification Level for Diyala River Basin in Iraq," *Iraqi Journal of Science*, pp. 1759-1767, 2016.

[22] S. K. Yadav, and S. K. Singh, "Morpho-tectonic assessment of Central Northern escarpment of Peninsular India, based on tectonically sensitive geomorphic indices," *J Physical Geography,* vol. 43, no. 6, pp. 753-783, 2022. https://doi.org/10.1080/02723646.2021.1899478.

[23] P. G. Silva, J. Goy, C. Zazo, and T. Bardají, "Fault-generated mountain fronts in southeast Spain: geomorphologic assessment of tectonic and seismic activity," *J Geomorphology,* vol. 50, no. 1-3, pp. 203-225, 2003. https://doi.org/10.1016/S0169-555X(02)00215-5.

[24] M. A. Bhat, T. Dar, and B. S. Bali, "Morphotectonic analysis of Aripal Basin in the North-Western Himalayas (India): An evaluation of tectonics derived from geomorphic indices," *Quaternary International,* vol. 568, pp. 103-115, 2020. https://doi.org/10.1016/j.quaint.2020.10.032.

[25] P. K. Gautam, D. S. Singh, D. Kumar, and A. K. Singh, "A GIS-based Approach in Drainage Morphometrie Analysis of Sai River Basin, Uttar Pradesh, India," *J Journal of the Geological Society of India,* vol. 95, no. 4, pp. 366-376, 2020. https://doi.org/10.1007/s12594-020-1445-9.

[26] R. T. Cox, "Analysis of drainage-basin symmetry as a rapid technique to identify areas of possible Quaternary tilt-block tectonics: an example from the Mississippi Embayment," *J Geological society of america bulletin,* vol. 106, no. 5, pp. 571-581, 1994. https://doi.org/10.1130/0016-7606(1994)106<0571:AODBSA>2.3.CO;2.

[27] J. T. Hack, "Stream-profile analysis and stream-gradient index," *Journal of Research of the us Geological Survey,* vol. 1, no. 4, pp. 421-429, 1973.

[28] [R. El Hamdouni, C. Irigaray, T. Fernández, J. Chacón, and E. Keller, "Assessment of relative active tectonics, southwest border of the Sierra Nevada (southern Spain)," *J Geomorphology,* vol. 96, no. 1-2, pp. 150-173, 2008. https://doi.org/10.1016/j.geomorph.2007.08.004.

[29] B. Gailleton, S. M. Mudd, F. J. Clubb, D. Peifer, and M. D. Hurst, "A segmentation approach for the reproducible extraction and quantification of knickpoints from river long profiles," *J Earth Surface Dynamics,* vol. 7, no. 1, pp. 211-230, 2019. https://doi.org/10.5194/esurf-7-211-2019.

[30] M. F. Ahmed, J. D. Rogers, and E. H. Ismail, "Knickpoints along the upper Indus River, Pakistan: An exploratory survey of geomorphic processes," *J Swiss Journal of Geosciences,* vol. 111, pp. 191-204, 2018. https://doi.org/10.1007/s00015-017-0290-3.

[31] E. Kusratmoko, A. Wibowo, and A. A. Kurnia, "Changes in the Value of Sinuosity Index in Komering River Channel, Province South Sumatera Years 1990-2016." p. 012024. https://doi.org/10.1088/1755-1315/338/1/012024.

[32] K. Hjerdt, J. McDonnell, J. Seibert, and A. Rodhe, "A new topographic index to quantify downslope controls on local drainage," *J Water resources research,* vol. 40, no. 5, 2004. https://doi.org/10.1029/2004WR003130.

[33] A. H. Al-Sulttani, and A. A. Beg, "Hypsometric analysis of Al-Adhaim Basin using a new GIS-technique," *The Iraqi Geological Journal*, pp. 154-170, 2020. https://doi.org/10.46717/IGJ.53.2B.8RS-2020.09.08.

[34] A. A. F. Beg. "Morphometric analysis toolbox used with ArcGIS desktop v.10.X," https://arcg.is/1bO8r51.

[35] P. K. Gautam, and A. K. Singh, "Evaluation of active tectonic features of Nandakini River Basin, Lesser Himalaya, India by using morphometric indices: A GIS approach," *Advances in Environmental and Engineering Research,* vol. 4, no. 1, pp. 1-24, 2023. https://doi.org/10.18517/ijaseit.8.6.6089.

[36] J. A. Zinck, "Physiography and soils," *J ITC Lecture Notes SOL,* vol. 41, pp. 1988, 1988.

[37] E. Mosavi, and M. Arian, "Neotectonics of Kashaf Rud River, NE Iran by Modified Index of Active Tectonics (MIAT)," *J International Journal of Geosciences,* vol. 6, no. 07, pp. 776, 2015. https://doi.org/10.4236/ijg.2015.67063.

[38] D. Gentana, N. Sulaksana, E. Sukiyah, and E. Yuningsih, "Index of active tectonic assessment: quantitative-based geomorphometric and morphotectonic analysis at way Belu drainage basin, Lampung Province, Indonesia," *International Journal of Advanced Science Engineering Information Technology,* vol. 8, no. 6, pp. 2460-2471, 2018. https://doi.org/10.18517/ijaseit.8.6.6089.

[39] A. A. F. Beg, "Morphometric Toolbox: A New Technique in Basin Morphometric Analysis Using ArcGIS," *Global Journal of Earth Science*

and Engineering, vol. 2, pp. 21-30, 2015. https://doi.org/10.15377/2409-5710.2015.02.02.1.

[40] N. A. Aziz, Z. Abdulrazzaq, and M. N. Mansur, "GIS-BASED WATERSHED MORPHOMETRIC ANALYSIS USING DEM DATA IN DIYALA RIVER, IRAQ," *The Iraqi Geological Journal*, pp. 36-49, 2020/03/29, 2020. https://doi.org/10.46717/igj.53.1C.3Rx-2020.04.03.

[41] T. H. Kadhim, and M. S. Al-kubaisi, "Relative tectonics activity assessment of diyala river area using lithological strength ratio and morphometric indices," *Bulletin of Pure & Applied Sciences- Geology,* vol. 41f, no. 1, pp. 115-128, 2022.

[42] A. T. Othman, and A. A. Omar, "Evaluation of relative active tectonics by using geomorphic indices of the Bamo anticline, Zagros Fold-Thrust Belt, Kurdistan Region of Iraq," *Heliyon,* vol. 9, no. 7, 2023. https://doi.org/10.1016/j.heliyon.2023.e17970.

[43] Z. Elias, V. K. Sissakian, and N. Al-Ansari, "Assessment of the tectonic activity in northwestern part of the Zagros Mountains, northeastern Iraq by using geomorphic indices," *Geotechnical and geological engineering,* vol. 37, no. 5, pp. 3995-4007, 2019. https://doi.org/10.1007/s10706-019-00888-z.

[44] L. H. Abdullah, H. S. Al Daghastani, and A. K. S. Bety, "Evaluation of neotectonic activity using watershed geomorphic analysis: A case study in the west of Dokan Lake, Kurdistan Region, Iraq," *Heliyon,* vol. 9, no. 2, 2023. http://dx.doi.org/10.1016/j.heliyon.2023.e13187.